

In-medium dependence and Coulomb effects of the pion production in heavy ion collisions

V.S. Uma Maheswari, C. Fuchs, Amand Faessler, L. Sehn, D.S. Kosov, Z. Wang

*Institut für Theoretische Physik der Universität Tübingen, D-72076 Tübingen,
Germany*

Abstract

The properties of the high energy pions observed in heavy ion collisions, in particular in the system Au on Au at 1 GeV/nucleon are investigated. The reaction dynamics is described within the Quantum Molecular Dynamics (QMD) approach. It is shown that high energy pions freeze out early and originate from the hot, compressed matter. N^* -resonances are found to give an importnat contribution toward the high energy tail of the pion. Further the role of in-medium effects in the description of charged pion yield and spectra is investigated using a microscopic potential derived from the Brueckner G-matrix which is obtained with the Reid soft-core potential. It is seen that the high energy part of the spectra is relatively more suppressed due to in-medium effects as compared to the low energy part. A comparision to experiments further demonstrates that the present calculations describe reasonably well the neutral (TAPS) and charged (FOPI) pion spectra. The observed energy dependence of the π^-/π^+ ratio, i.e. deviations from the isobar model prediction, is due to Coulomb effects and again indicate that high energy pions probe the hot and dense phase of the reaction. These findings are confirmed independently by a simple phase space analysis.

Key words: Pion spectra, isospin dependence, π^-/π^+ ratios, QMD

PACS numbers: **25.75.+r**

1 Introduction

Heavy ion collisions play a vital role in the quest for the nuclear equation of state, since a hot and dense nuclear matter phase is created, though transiently, in heavy ion collisions. In a typical intermediate energy reaction, for e.g. Au+Au at 1 GeV/A, matter gets compressed to densities of about two to three times the normal nuclear matter density ρ_0 and the maximum temperature attained in this central zone is supposed to reach values of few tens to about 100 MeV [1–3].

The investigation of particle production is a well established approach to probe the nuclear matter under these extreme conditions [4–6]. At incident energies around 1 GeV/A the pion production is the dominant channel by which the hot, compressed matter de-excites. Pion spectra at these relativistic energies have been measured at GSI (FOPI [7], KaoS [8,9], TAPS [10,11]) and LBL [4,5]. Unlike at lower energies the spectra show non-thermal slopes, i.e. one needs a superposition of two Maxwell-Boltzmann distributions to describe the data [5,7,9,11–13]. The onset of the second slope roughly coincides with the threshold for the Δ -resonance. Therefore, the resonance production and its subsequent decay into pions is considered to be important for an understanding of the excited nuclear matter. For this reason, in addition to the Δ -channel we include one-pion and two-pion decays of N^* -resonances and the respective one-pion reabsorption process. The role of these resonances in the production of the high energy pions is analysed in this work. Furthermore, recent measurements indicate that the high energy pions freeze out early, particularly when emitted perpendicular to the reaction plane [8,14]. Therefore, these pions most likely probe the early phase of the collision. Hence, a study of subthreshold pions is of current interest and is being actively pursued by both experimentalists and theoreticians.

As compared to the nature of subthreshold pions, the properties of the low energy pions, which are interpreted to be originating from Δ -decay, are relatively well understood within transport model approaches. However, one finds that the transport models such as QMD and BUU, in general, overestimate the charged pion yields as well as the low energy part of the spectra [7,15]. In this context, one has to keep in mind that the nuclear mean field, in particular, the respective momentum dependence of the interaction has large effects on various dynamical observables [16–18]. In most of the previous studies on pion production a nuclear mean field derived from effective phenomenological interactions, such as the Skyrme forces, have been applied [3,7,15,19,20]. However, a more realistic description of baryon dynamics in the hot and compressed phase of nuclear matter is possible within the framework of Brueckner theory where the nuclear mean field is derived microscopically from the G-matrix obtained by solving either the Bethe-Goldstone or the Bethe-Salpeter equation. With these realistic forces one finds in general an enhancement of the repulsive part of the nuclear interaction which originates from the strong momentum dependence of the G-matrix [16,17,21,22]. Since observables such as nuclear flow are found to be sensitive to the use of realistic forces [17,23,24], it is a worthwhile task to analyse the role of in-medium effects in the description of pionic observables at SIS energies. Therefore, in the present work, we also investigate the effect of the Brueckner G-matrix potential on pion multiplicities and spectra and then compare to the results obtained with the standard Skyrme interaction.

Another interesting aspect of the pion production observed in heavy ion col-

lisions is its charge dependence [25–29]. In the case of heavy systems such as Au one finds [7,9] for the total abundancies as a general law $\sigma(\pi^-) > \sigma(\pi^0) > \sigma(\pi^+)$. The two principal effects contributing to the observed charge dependence are the isospin dependence of the pion production cross sections and the Coulomb force. Since most of the pions observed at bombarding energies around 1 GeV/A originate from the decay of Δ -resonances, one can determine the isospin effect in a simple isobar model [6,30,31], which depends only on the Z/A ratio of the colliding systems and is independent of the pion energy. However, in Refs. [7,9] deviation from the behaviour predicted by the isobar model have been observed. The observed energy dependence of the π^-/π^+ ratio is then essentially due to the other factor, i.e. the Coulomb effect which modifies the pion momentum and the available phase space [28]. As mentioned in Ref. [32] one can moreover use the energy dependence of this ratio to estimate the size of the pion emitting source and thereby the density of the participant zone probed by the observed pions. This provides us with an alternative approach to investigate the nature of the subthreshold pions. To study this aspect, we take into account the Coulomb interaction between the baryons and the charged pions. This contributes toward the real part of the pion optical potential. Another contribution arises from the effect of nuclear medium on the pion dispersion relation, i.e. from collective ΔN^{-1} and NN^{-1} excitations. However, it is shown in a recent study [33] that only weak corrections, i.e. a small in-medium pion-nucleus potential, are required in order to obtain a realistic description of pionic observables. In addition, also in other works [34,35] it was found that the high energy part of the pion spectrum is not much affected by these medium corrections. A more sophisticated treatment of collective pionic excitations within the transport approach was proposed in Ref.[36] which was subsequently applied to heavy ion collisions in Ref.[37]. However, as discussed in Ref.[38], it is rather questionable if the simple ΔN^{-1} (and NN^{-1}) model yields a reliable pion dispersion relation. Further, the results of Ref.[37] indicate that the influence of collective excitations on pionic observables is small and tends to enhance the pion yields with respect to the standard approaches and the experimental findings. Hence, we omit such colective medium effects on the charge dependence of pion production in the present work.

Here we mainly focus upon the aforesaid aspects and investigate them using the Quantum Molecular Dynamics (QMD) model [39]. The essentials of the QMD model is briefly introduced in section 2. Results obtained are discussed in detail in section 3. Finally, we summarize our findings in section 4.

2 QMD model

Quantum molecular dynamics is a semiclassical transport model which accounts for relevant quantum aspects like the Fermi motion of the nucleons, stochastic scattering processes including Pauli blocking in the final states, the creation and reabsorption of resonances and the particle production. A detailed description of the QMD approach can be found in Refs. [17,39].

The time evolution of the individual nucleons is thereby governed by the classical equations of motion

$$\frac{\partial \vec{p}_i}{\partial t} = -\frac{\partial H}{\partial \vec{q}_i} \quad , \quad \frac{\partial \vec{q}_i}{\partial t} = \frac{\partial H}{\partial \vec{p}_i} \quad (1)$$

with the classical N -body Hamiltonian H

$$H = \sum_i \sqrt{\vec{p}_i^2 + M_i^2} + \frac{1}{2} \sum_{\substack{i,j \\ (j \neq i)}} \left(U_{ij} + U_{ij}^{\text{Yuk}} + U_{ij}^{\text{Coul}} \right) . \quad (2)$$

The Hamiltonian, Eq. (2), contains mutual two- (and three-) body potential interactions which are finally determined as classical expectation values from local Skyrme forces U_{ij} supplemented by a phenomenological momentum dependence and an effective Coulomb interaction U_{ij}^{Coul} ,

$$U_{ij} = \alpha \left(\frac{\rho_{ij}}{\rho_0} \right) + \beta \left(\frac{\rho_{ij}}{\rho_0} \right)^\gamma + \delta \ln^2 \left(\epsilon |\vec{p}_i - \vec{p}_j|^2 + 1 \right) \frac{\rho_{ij}}{\rho_0}, \quad (3)$$

$$U_{ij}^{\text{coul}} = \left(\frac{Z}{A} \right)^2 \frac{e^2}{|\vec{q}_i - \vec{q}_j|} \text{erf} \left(\frac{|\vec{q}_i - \vec{q}_j|}{\sqrt{4L}} \right), \quad (4)$$

where ρ_{ij} is a two-body interaction density defined as

$$\rho_{ij} = \frac{1}{(4\pi L)^{\frac{3}{2}}} e^{-(\vec{q}_i - \vec{q}_j)^2 / 4L}, \quad (5)$$

and erf is the error function. The parameters $\alpha, \beta, \gamma, \delta, \epsilon$ of the Skyrme interaction, Eq. (3), are determined in order to reproduce simultaneously the saturation density ($\rho_0 = 0.16 \text{ fm}^{-3}$) and the binding energy ($E_B = -16 \text{ MeV}$) for normal nuclear matter for a given incompressibility K_∞ as well as the correct momentum dependence of the real part of the nucleon-nucleus optical potential [17,40]. In the present calculations we use a soft equation of state with $K_\infty = 200 \text{ MeV}$ including the momentum dependent interaction (SMD),

Eq. (3). The Yukawa-type potential U_{ij}^{Yuk} in Eq. (2) mainly serves to improve the surface properties and the stability of the initialized nuclei.

Nucleons while propagating shall collide stochastically, if the distance between the centroids of the two Gaussian wavepackets is less than $d_{\min} = \sqrt{\sigma_{\text{tot}}(\sqrt{s})/\pi}$. This collision process is implemented using Monte Carlo method and the effect of Pauli exclusion principle is duly taken into account. For the inelastic nucleon-nucleon channels we include the $\Delta(1232)$ as well as the $N^*(1440)$ resonance. In the intermediate energy range the resonance production is dominated by the Δ , however, the N^* yet gives non-negligible contributions to the high energetic pion yield [41]. The resonances as well as the pions originating from their decay are explicitly treated, i.e. in a non-perturbative way and all relevant channels are taken into account. In particular we include the resonance production and rescattering by inelastic NN collisions, the one-pion decay of Δ and N^* and the two-pion decay of the N^* and one-pion reabsorption processes. (For details see Ref. [33].)

Pions thus produced are propagated according to the same equations of motion given in Eq.(1). The Hamiltonian corresponding to pions is given as

$$H_\pi = \sum_{i=1}^{N_\pi} \left(\sqrt{\vec{p}_i^2 + m_\pi^2} + V_i^{\text{Coul}} \right). \quad (6)$$

The Coulomb interaction V_i^{Coul} between the baryons the charged pions is given as

$$V_i^{\text{Coul}} = \sum_{j=1}^{N_b} \frac{e_i e_j}{| \vec{q}_j - \vec{q}_i |}, \quad (7)$$

where N_b and N_π are respectively the total number of baryons including charged resonances and pions at a given time t . Thus, pion propagation at the intermediate and final stages is guided essentially by the Coulomb effect.

3 Results and Discussions

3.1 High energy pions and role of N^* resonances

Since the observation that high energy pions freeze out early when emitted perpendicular to the reaction plane, the focus has been to establish, both experimentally and theoretically that these high energy pions probe the hot and dense phase of the collision. Hence, we analyse the properties of high

energy pions and the effect of heavier baryon resonances, such as the $N^*(1440)$, in this regard. Here we adopt the phenomenological Skyrme interaction SMD.

For this purpose we calculated the total pion multiplicity in Au+Au collision at 1 GeV/A corresponding to the *minimum bias* condition. According to Ref. [7], we choose $b_{\text{max}}=11$ fm. Results obtained are shown in Fig.1 as a function of pion transverse momentum p_t and pion freeze out time t_{freeze} , i.e. the time after which pions do no more interact via inelastic scattering processes. It can be seen that most of the pions are in the region $p_t \leq 200$ MeV/c and $t_{\text{freeze}} \sim 30$ fm/c. In order to project out the high energy pions, we normalised the pion multiplicity $M(p_t)$ obtained for each value of p_t by its maximum value $M_{\text{max}}(p_t)$. The normalized multiplicity is shown in Fig.2, where it is seen that the peak value shifts toward early times as the value of p_t is increased. For example, pions with $p_t \sim 200$ MeV/c freeze out at $t \sim 30$ fm/c; whereas for $p_t \sim 500$ MeV/c one finds $t_{\text{freeze}} \sim 20$ fm/c. This directly shows that high- p_t pions originate from early times. In order to relate these pions with the compressed early phase, we calculated the total baryon density ρ_B in a sphere of 2 fm radius around the collision centre with impact parameter $b=1$ fm. The time evolution of the ρ_B/ρ_0 is shown in Fig.3, where the $\rho_0 = 0.16 \text{ fm}^{-3}$ is the normal nuclear matter density. The maximum density is achieved at about 25 fm/c and is about $2\rho_0$. Over the time span $10 \leq t \leq 30$ fm/c the density in the collision center is at least ρ_0 , and this time span may then be identified with the hot, compressed participant phase. Thus, from this analysis we find similar to a previous study using hard equation of state and only Δ -resonances [20] that high energy pions with $t_{\text{freeze}} \sim 20$ fm/c pertain to the early phase of the collision, when the matter is compressed to about $2\rho_0$.

For the sake of completeness we show in Fig.4 for two impact parameters, $b = 0 \text{ fm}$ and $b = 6 \text{ fm}$ the collision configuration, i.e. the evolution of the average distance $\Delta R = R_P - R_T$ between the centres of the colliding nuclei where R_P and R_T represent the average position of the centres of the projectile and target nuclei, respectively. The collision centre is at the zero of the Y-axis. The curves representing R_P are in the positive Y-axis plane and those representing R_T are in the negative Y-axis plane. The two dotted lines correspond to the sharp density radii of the two colliding nuclei. Thereby, it can be seen that at about $4 \text{ fm}/c$ when the curves corresponding to R_P and R_T intersect the dotted lines the nuclei come in contact, i.e. this represents the touching configuration. Further, for very central collisions the time span upto $\sim 25 \text{ fm}/c$ pertains to the compression stage, and beyond which the expansion process begins. Hence, the maximum density or compression is attained at about $25 \text{ fm}/c$, which is consistent with the results shown in Fig.3. It may also be noted that for finite values of impact parameter b , one has at the time of maximum compression $\Delta R = b$.

To illustrate the contribution of high energy pions from N^* resonances, we have

compared in Fig.5 the total pions originating from Δ - resonance to those from N^* . The pion multiplicity linearly weighted by impact parameter b is shown as a function of b . It is seen that the contribution from N^* -resonances irrespective of the nature of the collision, i.e. central, semi-central or peripheral, is about 5%. Though their multiplicity is small, they play an important role as most of them originate from early times. This aspect is illustrated in Fig.6 where we have plotted M_π^Δ/M_π as a function of pion freeze out time t_{freeze} . The total number of pions from Δ and N^* are labelled as M_π^Δ and $M_\pi^{N^*}$ respectively, with $M_\pi = M_\pi^\Delta + M_\pi^{N^*}$. Interestingly, the maximum contribution from N^* (about 8%) occurs at $t_{\text{freeze}} \sim 20$ fm/c. It maybe recalled here that pions with this value of t_{freeze} pertain to the dense phase with $\rho_B \geq 2\rho_0$. Therefore, the majority of the N^* pions originate from early times and hence are most likely high energetic ones.

To demonstrate this aspect we calculated the neutral pion spectrum at midrapidity under the *minimum bias* condition. (We have chosen π^0 so that the high energy tail of the spectrum is not distorted by Coulomb effects.) Results obtained are shown in Fig.7 alongwith the π^0 spectrum calculated only with N^* pions. In the same figure, we have also shown the TAPS data for comparison. Due to a recent experimental analysis the data given in [11] have to be renormalized by factor 0.6 [15]. It is clearly seen that the N^* contribution to the high energy tail is by a factor of about two more than its contribution toward low energy pions. This is in agreement with a recent study [15] based on the BUU model where it was shown, though for a different system at a higher energy, that contributions from baryonic resonances like $N^*(1440, 1520, 1535)$ and $\Delta(1600)$ are significant over the high energy tail of the pion spectra. Moreover, the $\pi^0(N^*)$ spectra in Fig.7 portrays two distinct slopes and the slope parameter T extracted from the high energy part is relatively higher than the one obtained from the high energy part of the total π^0 spectrum. This again establishes that N^* pions pertain to earlier times as compared to those from Δ . Therefore, it may be said that pions from N^* need to be included for a consistent description of the high energy tail.

3.2 In-medium effects on charged pions

As discussed in Introduction, we now investigate the effect of microscopically determined nuclear mean field on obsevables such as pion yield and spectra. (All data shown in this section are taken from Ref. [7].)

For this purpose, the G-matrix is obtained by solving the Bethe-Goldstone equation

$$G = V + V \frac{Q}{\omega - H_0 + i\eta} G \quad (8)$$

where Q is the Pauli operator which forbids nucleons from scattering into occupied states. The bare NN interaction V is taken to be the Reid soft-core interaction and H_0 is the single particle energy [42,43]. Thus, the G-matrix accounts for the most relevant medium effects in nuclear matter. The mean field potential U_{GMAT} is derived from the G-matrix as [16,17]

$$U_{\text{GMAT}}(\rho, \vec{p}) = 4 \int_F \frac{d^3 p'}{(2\pi)^3} (\vec{p}, \vec{p}' | G(\rho) | \vec{p}, \vec{p}') . \quad (9)$$

For the purpose of a simple application within the QMD model the potential is parametrized in a Skyrme-like form

$$U_{\text{GMAT}}(\rho, p) = a_1 \left(\frac{\rho}{\rho_o} \right) + a_2 \left(\frac{\rho}{\rho_o} \right)^{a_3} + a_4 \ln^2[a_5 p^2 + 1] \left(\frac{\rho}{\rho_o} \right)^{a_6} . \quad (10)$$

The coefficients a'_i s were determined from a fit of Eq. (10) to the microscopically calculated values of U_{GMAT} , Eq.(9), within the density range of $0 \leq \rho \leq 2\rho_o$ and for momenta $p \leq 500 \text{ MeV}/c$. The momentum dependence of so-determined potential at $\rho = \rho_o$ is shown in Fig.8 alongwith the one obtained from the phenomenological Skyrme force using Eq. (3). (Calculations done with the Skyrme force and the G-matrix potential are hereafter referred to as SMD and GMAT, respectively.) For comparison, we have also shown the potential as obtained by Li and Machleidt [21] using the Dirac-Brueckner approach. It can be seen that the nuclear mean field derived from the non-relativistic G-matrix is slightly more attractive at low momenta and less repulsive at high momenta compared to the one obtained from the relativistic G-matrix. However, the general behaviour is quite similar. The prominent feature of the realistic G-matrix interaction is the significantly stronger momentum dependence as compared to the Skyrme force. In a recent study [44] on the effect of realistic forces on collective nucleon flow it was found that the relativistic (Dirac-Brueckner) and non-relativistic (Brueckner) approaches yield quite similar results when applied to heavy ion collisions. However, the differences to phenomenological interactions (Skyrme or Walecka model) are significant. Thus, it is of interest to investigate the sensitivity of pionic observables to realistic forces. In order to be as consistent as possible, we have also considered the effect of in-medium cross sections [16,17] in the elastic NN channel for center-of-mass momentum $p < 500 \text{ MeV}/c$, which are derived from the same microscopic G-matrix potential using the two-Fermi-sphere approach. However, the effect of the in-medium cross section on the pion yield has been found to be small compared to that of the mean field and is therefore not discussed in detail in the following.

Results obtained for the π^+ multiplicity is plotted in Fig.9 as a function of the participant nucleons A_{part} . It is seen that the theoretical calculation

overestimate the data of the Au system by about 50% at small impact parameters. In this context we want to mention that the pion multiplicities obtained by other groups for central $Au + Au$ reaction at 1 GeV/A, using QMD [3,7] or BUU [19,37] models, differ only within about 10% with our results. Thus, this overestimation at small impact parameters seems to be a general feature of present transport calculations. However, the theoretical prediction is more in agreement with the experimentally derived Harris systematics [45]. It may also be noted that the Harris systematics while it overpredicts as compared to the FOPI data in the case of heavy system such as Au is in good agreement with the data for smaller system like Ni [46]. We have also shown in Fig.10, the rapidity distribution obtained under minimum bias condition. In both SMD and GMAT calculations one finds at midrapidity a overestimation of about 30%, as compared to the data. Similar features are also observed in the case of π^- .

To see the effect upon momentum distribution, we calculated the charged pion spectra. Results obtained with both SMD and GMAT potentials are then compared in Figs.11 and 12 to the corresponding FOPI data. The overall agreement with the observed spectra is reasonably good. In particular, one finds that with the inclusion of in-medium effects, there is a slight reduction over the low energy part thus coming closer to the data. But, a larger effect is observed over the high energy part where the subthreshold pions get quite suppressed indicating the importance of resonances heavier than Δ and N^* . Thus, one finds that, as compared to the high energy part, the low energy part is not too much affected by the strong momentum dependence of GMAT potential which may be due to the fact that low energy pions are frequently reabsorbed. For a more complete description of pion yields and spectra, one probably needs to include the in-medium effects in the inelastic NN channel as well. In addition, a possible reason for the overestimation over the low energy part can be the life-time of the resonances involved. (Some indication towards this can be inferred from Fig.1, where one finds that even at 60 fm/c , resonances are still decaying into pions though their multiplicity is quite small.) E.g. in Ref.[47] an alternative treatment of the resonance lifetime has been proposed, which is based on more quantum mechanical aspects. However, it is still unclear at the moment how such a description should be applied consistently in transport simulations.

3.3 π^-/π^+ ratio and Coulomb effect

We had demonstrated theoretically that high energy pions originate from the early phase of the collision. Here, using the observed energy dependence of π^-/π^+ ratio, we re-iterate that high energy pions do probe the hot and dense matter.

It is known that the two principal effects contributing toward the observed charged dependence of pion production, i.e. $\sigma(\pi^-) > \sigma(\pi^0) > \sigma(\pi^+)$, are the isospin dependence of the pion production cross sections and the Coulomb force. As most of the pions observed are from Δ -resonance, one can determine the effect of isospin. Using the isobar model [6] one finds for pion originating from Δ -decay the general relation

$$\sigma(\pi^-)/\sigma(\pi^0) = \frac{5N^2 + NZ}{N^2 + 4NZ + Z^2} \quad , \quad \sigma(\pi^+)/\sigma(\pi^0) = \frac{5Z^2 + NZ}{N^2 + 4NZ + Z^2} \quad (11)$$

For the Au+Au system we obtain the ratios $\pi^- : \pi^0 : \pi^+ = 1.37 : 1 : 0.71$ for the repetitive multiplicities. Therefore, one has $\pi^-/\pi^+ = 1.95$. For pions from N^* the isobar model yields $\pi^-/\pi^+ = 1.70$. Since these relations are globally valid, i.e. independent of the pion energy, the observed energy dependence of the π^-/π^+ ratio must be due to the Coulomb potential energy V_C [20,19]. This is illustrated in Fig. 13, where the ratio of the calculated differential cross sections $\sigma_E(\pi^-)/\sigma_E(\pi^+)$ with $\sigma_E = d^2\sigma/(pE dp d\Omega)$ are compared with the observed one [7]. One finds that the overall behaviour of the measured ratios is well reproduced. In particular, over the low energy part both SMD and GMAT curves are quite similar. However, at higher energies $T_{c.m.} > 300$ MeV, i.e. $p_{c.m.} > 400$ MeV, the GMAT results show stronger fluctuation as compared to the SMD case, which may be due to the suppressed cross sections. Such strong fluctuations over high energy part are also apparent in the experimental data. Nevertheless, the trend in Fig.13 indicates that the results approach a constant value as the pion momentum $p_{c.m.}$ increases which is in agreement with the experimental findings.

The general features of the effect of the Coulomb force on the π^-/π^+ can be understood using a simple analytical model as described in Ref. [28]. Let p_0 and p be the initial and final momenta of a charged particle. Then the charged particle cross section $\sigma(p) \equiv d^3\sigma/d^3p$ can be related to the neutral particle cross section $\sigma_0(p) \equiv d^3\sigma_0/d^3p$ through the change of

$$\sigma(p) = \sigma_0(p_0(p)) \left| \frac{\partial^3 p_0}{\partial^3 p} \right|. \quad (12)$$

The two effects due to Coulomb force are the momentum shift $\delta p = p - p_0$ and the Coulomb phase space factor $\left| \partial^3 p_0 / \partial^3 p \right|$. Taking relativistic quantum corrections up to first order in $Z\alpha$ and in the limit $p \rightarrow \infty$, one has $\pm \delta p \sim V_C / \beta_p$ and $\left| \partial^3 p_0 / \partial^3 p \right| \sim 1 \pm V_C / p$, where $\beta_p = p/\omega_p$ and $\omega_p = \sqrt{p^2 + m_\pi^2}$. Omitting the phase space factor in Eq. (12) in the limit $p \rightarrow \infty$ the π^-/π^+ ratio is then given as

$$\frac{\sigma_{\pi^-}}{\sigma_{\pi^+}} \sim \frac{C_-}{C_+} \exp \left(-\frac{1}{T} [\omega_- - \omega_+] \right) \quad (13)$$

where $\omega_\pm^2 = p_\pm^2 + m_\pi^2$ and $p_\pm = p \mp \delta p$.

It is found experimentally that the high energy slopes of π^- and π^+ are very similar and hence the slope parameter T is the same for both positive and negative charged pions. Moreover, one finds Eq. (13) is independent of the momentum p and the ratio π^-/π^+ is in good approximation given by a constant determined by the Coulomb energy shift, i.e. by V_C . This is consistent with the experimental observation where one finds that the π^-/π^+ ratio approaches a constant value of about 0.93 in the high momentum limit. Therefore, the above approximate equation can be used in the high energy limit to estimate the Coulomb energy V_C . In addition we take the value of C_-/C_+ according to Eq. 11 to be 1.95 thus accounting for the isospin dependence of the cross sections. It may be noted that a very similar value ($C_-/C_+ = 1.94 \pm 0.05$) is obtained experimentally in the zero momentum limit [32]. Taking the slope parameter T to be 94.6 MeV [7] and the constant value of π^-/π^+ ratio to be 0.93 we obtain the Coulomb energy V_C to be about 35 MeV. The radius R of the pion emitting source is then estimated to be 4.5 fm with the assumption of a static uniform Coulomb field $V_C \sim Ze^2/R$ where the total number of participating charges Z is taken to be 110 as estimated in Ref. [32]. We also estimated the density $\rho \sim 3A/(4\pi R^3)$ of the participant zone to be about $4\rho_0$ where the total number of participants $A \simeq 197$ ($Z/79$). It may be noted that the estimation of ρ is about two times the value obtained from the actual simulation, see also Fig. 3. If we consider a more realistic value $\rho = 2\rho_0$ and using the fact that $V_C \simeq 35$ MeV we obtain $R = 6.7$. This then gives an idea about the order of magnitude of uncertainty present in the estimation of the pion source size R and the effective number of participating charges Z . From this simple analysis based on the observed energy dependence of the π^-/π^+ ratio, we find in support of our theoretical investigation that the high energy pions probe the hot, compressed phase of the collision. However, the empirical determination of the freeze-out radius from measured π^-/π^+ ratios [32] should be performed carefully. In this context, it may be noted that a recent analysis [29] of π^-/π^+ ratios measured in $Au + Au$ collision at 11 GeV/A and in $Pb + Pb$ at 158 GeV/A shows valley like structures in the minimum χ^2 plane rendering the determination of R and Z from the data difficult. Moreover, the scenario for the origin of high energy pions is probably not that of an equilibrated and thermalized source but rather that of two counterstreaming nuclear matter currents with high relative velocities and thus, e.g., Lorentz forces should be taken into account in such an analysis.

4 Summary

In this work we investigated the production of pions in $Au+Au$ collisions at 1 GeV/A using the QMD model. Focussing upon the high energy pions, we

showed that these subthreshold pions freeze out at early times when the matter is compressed to more than two times the saturation density. Hence, they probe the hot and dense phase of the nuclear reaction. One of the processes which can produce such energetic pions is the decay of baryonic resonances like the N^* . A detailed analysis shows that even though the multiplicity of pions from the decay of N^* is small compared to those from Δ -decay, i.e. about 5% of the total yield, they play an important role as most of them pertain to the early phase of the reaction. Further, it is found that N^* contribution toward high energy pions is by a factor of about two more than its contribution toward low energy pions. Therefore, pions from higher resonances like N^* need to be included for a consistent description of the high energy tail of the pion spectra.

Moreover, due to the importance of momentum dependence in the study of heavy ion collisions, we have also studied the role of in-medium effects by performing calculations with a microscopic nuclear mean field derived from the Brueckner G-matrix using the Reid soft-core interaction. It is found that calculated pion multiplicities, though they agree reasonably well with the Harris systematics overestimate the FOPI data at small impact parameters by about 50%. The use of realistic G-matrix interaction improves this situation, however, not to a sufficiently high extent. We then compared the charged pion spectra calculated with G-matrix and Skyrme potentials to the respective FOPI data. It is found that the high energy part gets relatively more suppressed by in-medium effects, as compared to the low energy part. Therefore, for a complete description of pion yield and spectra, one probably needs to consistently include in-medium effects both in the elastic and inelastic NN channels. In addition, an improved treatment of lifetime of resonances may also be warranted.

Finally, we investigated the isospin dependence of the pion production. The present calculations are able to reproduce the overall behavior of the measured π^-/π^+ ratios. Deviations from the simple isobar model originate from the Coulomb force. These deviations found for high energy pions indicate the influence of the Coulomb field on pions stemming from the high density phase. These findings are in qualitative agreement with a simple analysis based only on the observed π^-/π^+ ratios and the slopes of the respective spectra.

Acknowledgements

We thank D. Pelte for providing us with the FOPI data shown in this work.

References

- [1] R.K. Puri, N. Ohtsuka, E. Lehmann, A. Faessler, H.M. Martin, D.T. Khoa, G. Batko, and S.W. Huang, Nucl. Phys. A 536 (1992) 201.
- [2] T. Maruyama, W. Cassing, U. Mosel, S. Teis, and K. Weber, Nucl. Phys. A 573 (1994) 653.
- [3] S.A. Bass, C. Hartnack, H. Stöcker and W. Greiner, Phys. Rev. C 51 (1995) 3343.
- [4] S. Nagamiya, M.C. Lemarie, E. Moeller, S. Schnetzer, G. Shapiro, H. Steiner, and I. Tanihata, Phys. Rev. C 24 (1981) 971.
- [5] R. Brockmann *et al* , Phys. Rev. Lett. 53 (1984) 2012.
- [6] R. Stock, Phys. Rep. 135 (1986) 259.
- [7] D. Pelte and the FOPI Collaboration, Z. Phys. A 357 (1997) 215.
- [8] D. Brill and the KaoS Collaboration, Phys. Rev. Lett. 71 (1993) 336.
- [9] C. Müntz and the KaoS Collaboration, Z. Phys. A 352 (1995) 175.
- [10] L. Venema and the TAPS Collaboration, Phys. Rev. Lett. 71 (1993) 835.
- [11] O. Schwalb and the TAPS Collaboration, Phys. Lett. B 321 (1994) 20.
- [12] W. Bauer and B.A. Li, Phys. Lett. B 254 (1991) 335.
- [13] P. Braun-Munzinger, J. Stachel, J. P. Wessels, N. Xu, Phys. Lett. B 344 (1995) 43.
- [14] S.A. Bass, C. Hartnack, H. Stöcker and W. Greiner, Phys. Rev. Lett. 71 (1993) 1144.
- [15] S. Teis, W. Cassing, M. Effenberger, A. Hombach, U. Mosel, and Gy. Wolf, Z. Phys. A 356 (1997) 421.
- [16] J. Jaenicke, J. Aichelin, N. Ohtsuka, R. Linden and A. Faessler, Nucl. Phys. A 536 (1992) 201.
- [17] D.T. Khoa, N. Ohtsuka, M.A. Matin, A. Faessler, S.W. Huang, E. Lehmann and R.K. Puri, Nucl. Phys. A 548 (1992) 102.
- [18] C. Gale, G. F. Bertsch and S. Das Gupta, Phys. Rev. C 35 (1987) 1666;
J. Aichelin, A. Rosenhauer, G. Peilert, H. Stoecker and W. Greiner, Phys. Rev. Lett. 58 (1987) 1926;
G.M. Welke, M. Prakash, T.T.S. Kuo and S. Das Gupta, Phys. Rev. C 38 (1988) 2101;
F. Sebille, G. Royer, C. Gregoire, B. Remaud and P. Schuck, Nucl. Phys. A 501 (1989) 137.

- [19] S. Teis, W. Cassing, M. Effenberger, A. Hombach, U. Mosel, and Gy. Wolf, nucl-th/9701057.
- [20] S.A. Bass, C. Hartnack, H. Stöcker and W. Greiner, Phys. Rev. C 50 (1994) 2167.
- [21] G.Q. Li and R. Machleidt, Phys. Rev. C 48 (1993) 2707.
- [22] L. Sehn, C. Fuchs and A. Faessler, nucl-th/9701060, (Phys. Rev. C in press).
- [23] V. Ramillien et al, FOPI collaboration, Nucl. Phys. A 587 (1995) 802.
- [24] C. Fuchs, T. Gaitanos and H.H. Wolter, Phys.Lett. B 381 (1996) 23.
- [25] W. Benenson et al., Phys. Rev. Lett. 43 (1979) 683.
- [26] K.G. Libbrecht and S.E. Koonin, Phys. Rev. Lett. 43 (1979) 1581.
- [27] G. Bertsch, Nature 283 (1980) 280.
- [28] M. Gyulassy and S.K. Kauffmann, Nucl. Phys. A 362 (1981) 503.
- [29] T. Osada, S. Sano, M. Biyajima, and G. Wilk, Phys. Rev. C 54 (1996) R2167.
- [30] B.J. VerWest and R.A. Arndt, Phys. Rev. C 25 (1982) 1979.
- [31] T. Ericson and W. Weise, Pions and Nuclei, Carendon Press Oxford 1988.
- [32] H. Oeschler and the KaoS Collaboration, Proceedings on the Conference on "Modern physics at the turn of the millenium", Wilderness (South Africa) 1996.
- [33] C. Fuchs, L. Sehn, E. Lehmann, J. Zipprich and A. Faessler, Phys. Rev. C 55 (1997) 411.
- [34] W. Ehehalt, W. Cassing, A. Engel, U. Mosel and Gy. Wolf, Phys. Lett. B 298 (1993) 31.
- [35] L. Xiong, C.M. Ko and V. Koch, Phys. Rev. C 47 (1993) 788.
- [36] J. Helgesson and J. Randrup, Ann. Phys.(N.Y.) 244 (1995) 12; Nucl. Phys. A 597 (1996) 672.
- [37] J. Helgesson and J. Randrup, nucl-th/9705022, Phys. Lett.B in press.
- [38] C. Fuchs, L. Sehn, E. Lehmann, J. Zipprich and A. Faessler, Phys. Rev. C in press.
- [39] J. Aichelin, Phys. Rep. 202 (1991) 233.
- [40] J. Aichelin, H. Stöcker, Phys. Lett. B 176 (1986) 14.
- [41] V. Metag, Prog. Part. Nucl. Phys. 30 (1993) 75.
- [42] T. Izumoto, S. Krewald and A. Faessler, Phys. Lett. B 95 (1980) 16; Nucl. Phys. A 341 (1980) 319.

- [43] N. Othsuka, R. Linden, A. Faessler and F. B. Malik, Nucl. Phys. A 465 (1987) 550.
- [44] C. Fuchs, E. Lehmann, R.K. Puri, A. Faessler and H.H. Wolter, J. Phys. G 22 (1996) 131.
- [45] J. W. Harris et al, Phys. Rev. Lett. 58 (1987) 463.
- [46] D. Pelte and the FOPI collaboration, nucl-ex/9704009.
- [47] P. Danielewicz and S. Pratt, Phys. Rev. C 53 (1996) 249.

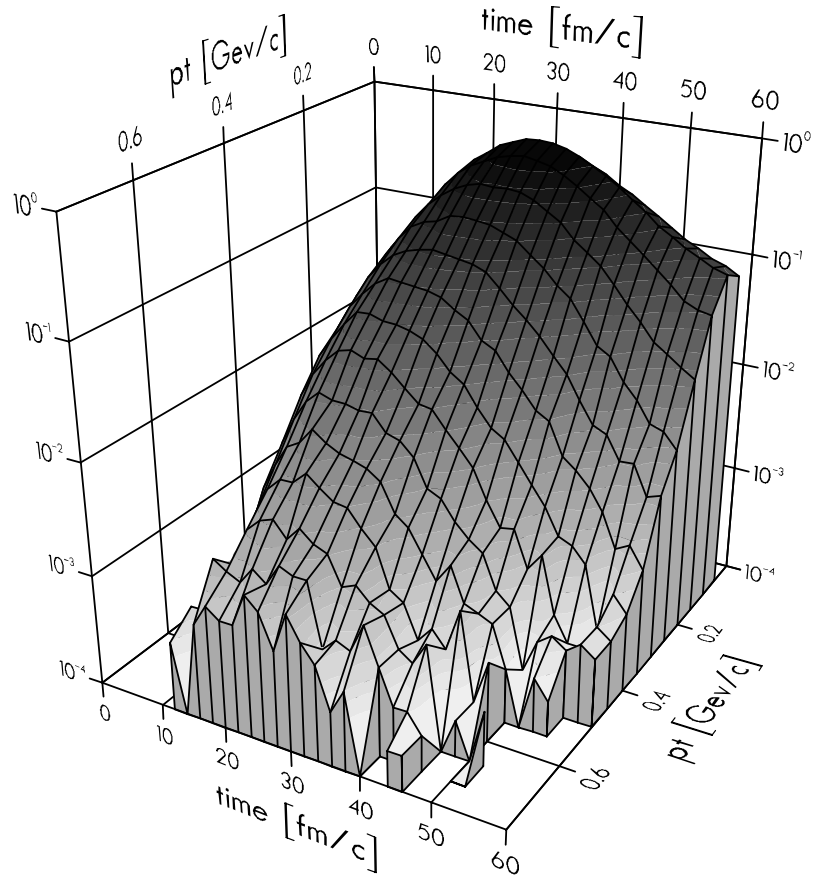


Fig. 1. Total pion multiplicity calculated with a Skyrme force (SMD) in Au+Au at 1 GeV/A under *minimum bias* condition is shown as a function of pion transverse momentum p_t and pion freeze out time t_{freeze} .

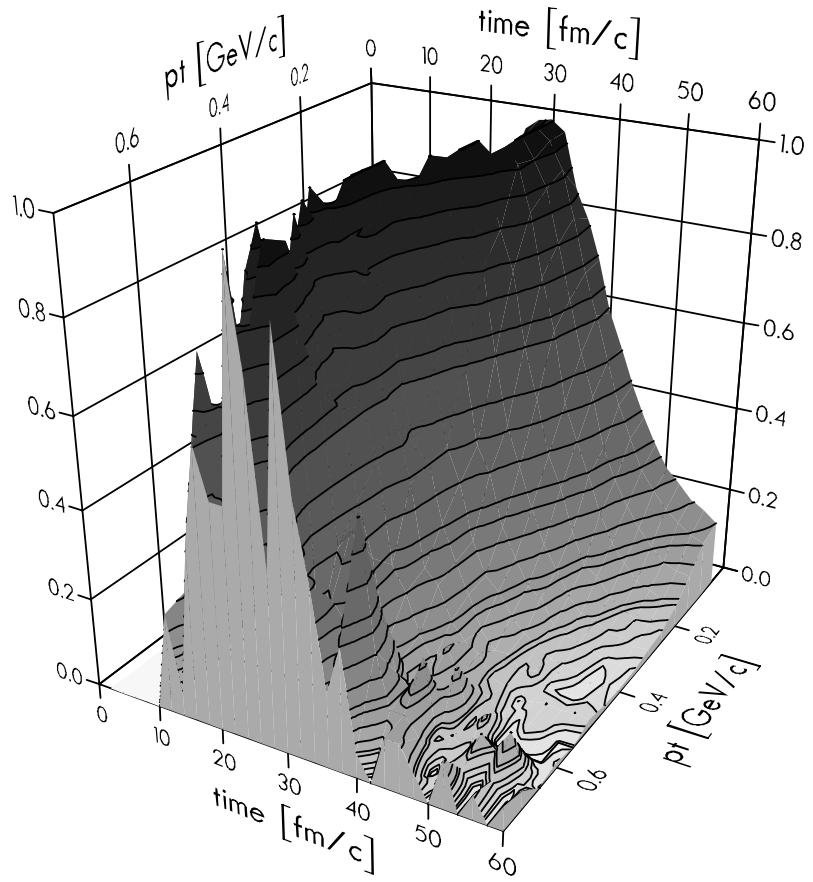


Fig. 2. Normalized pion multiplicity, i.e. the multiplicity calculated for each value of p_t is normalized by its maximum value, obtained in as the same reaction in Fig. 1 is shown as a function of pion transverse momentum p_t and pion freeze out time t_{freeze} .

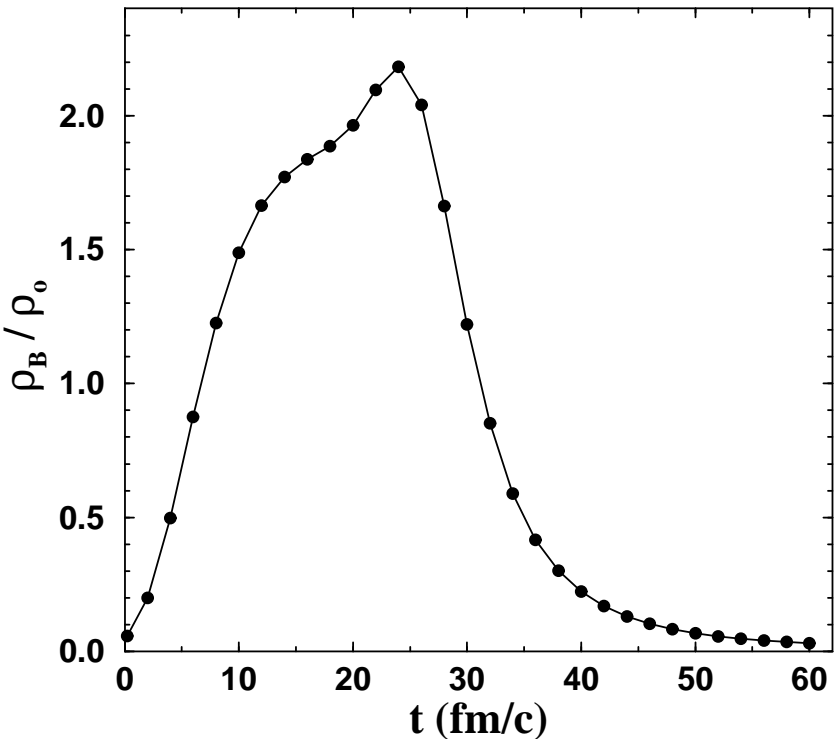


Fig. 3. Time evolution of the baryon density ρ_B in a central ($b=1$ fm) Au on Au reaction at 1 GeV/A. ρ_B is calculated with a Skyrme force (SMD) in a sphere of 2 fm radius around the collision center.

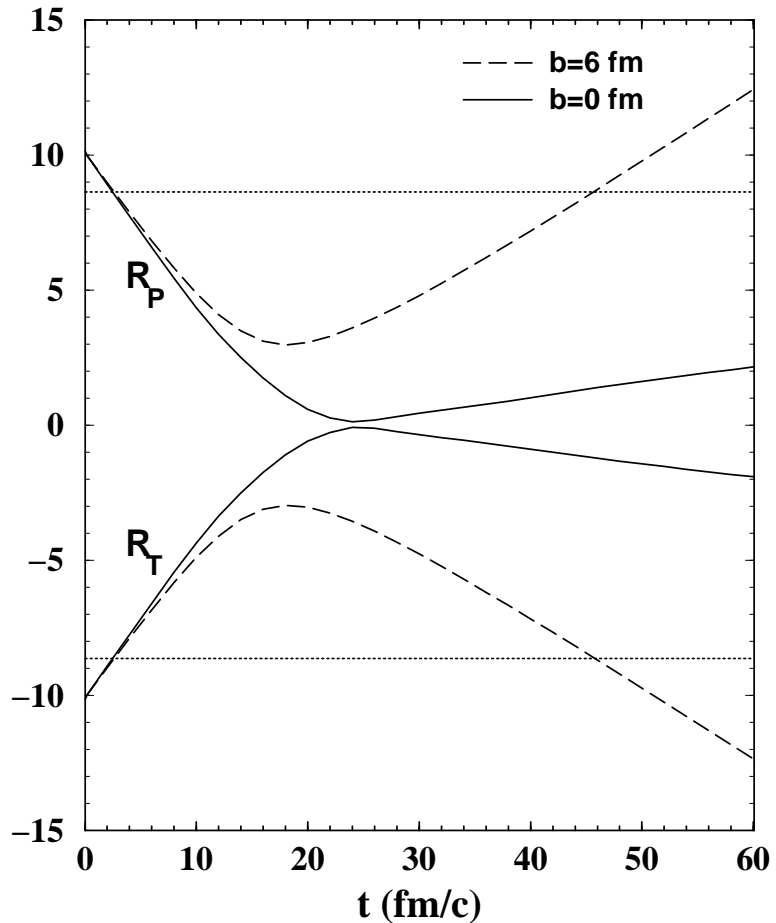


Fig. 4. Time evolution of the average distance $\Delta R = R_P - R_T$ between the centres of the two colliding nuclei ($Au + Au$) is shown for two impact parameters. R_P and R_T represent the average position of the centre of the projectile and target, respectively. Curves corresponding to R_P are in the positive Y-axis plane, and those for R_T are in the negative Y-axis plane. Zero of the ordinate corresponds to the collision centre. Dotted lines represent the sharp density radii of the two nuclei.

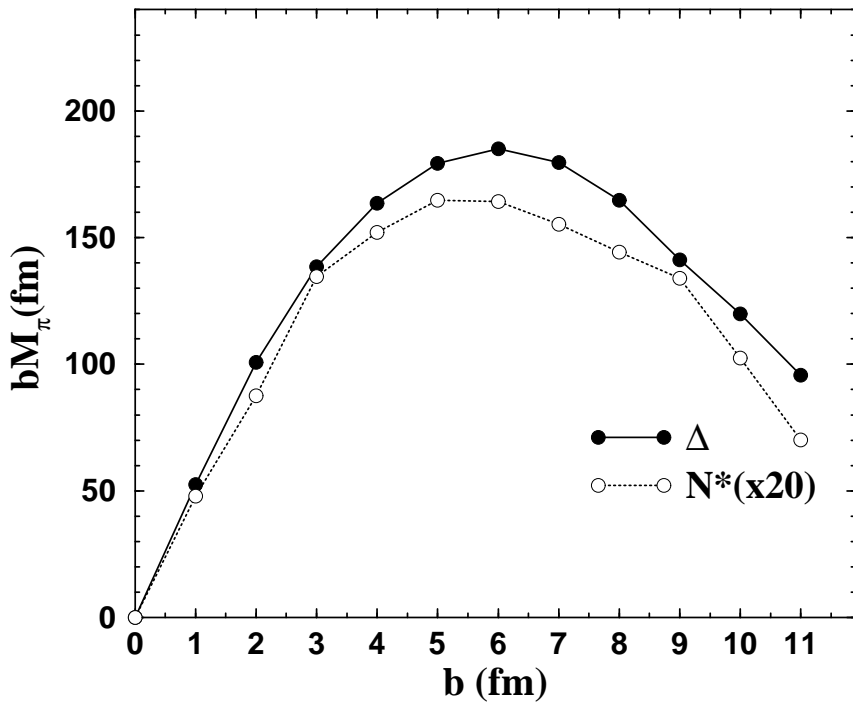


Fig. 5. The total multiplicity of pions calculated with a Skyrme force (SMD) originating from N^* -resonances is compared to those from Δ -resonances. The pion multiplicity M_π linearly weighted by the impact parameter b is shown as a function of b .

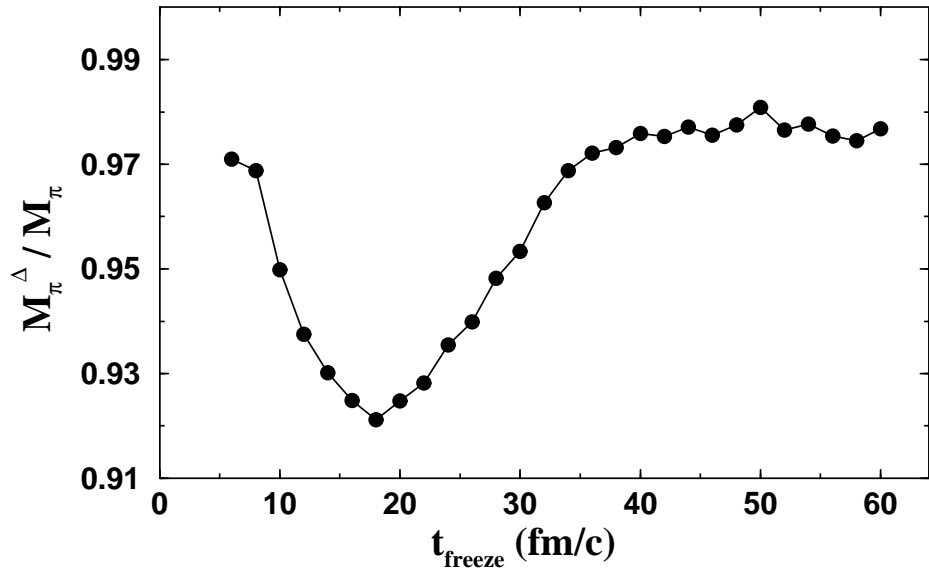


Fig. 6. The multiplicity of pions stemming from the decay of Δ -resonances M_π^Δ normalized to the total pion multiplicity M_π calculated with a Skyrme force (SMD) is shown as a function of the pion freeze-out time t_{freeze} .

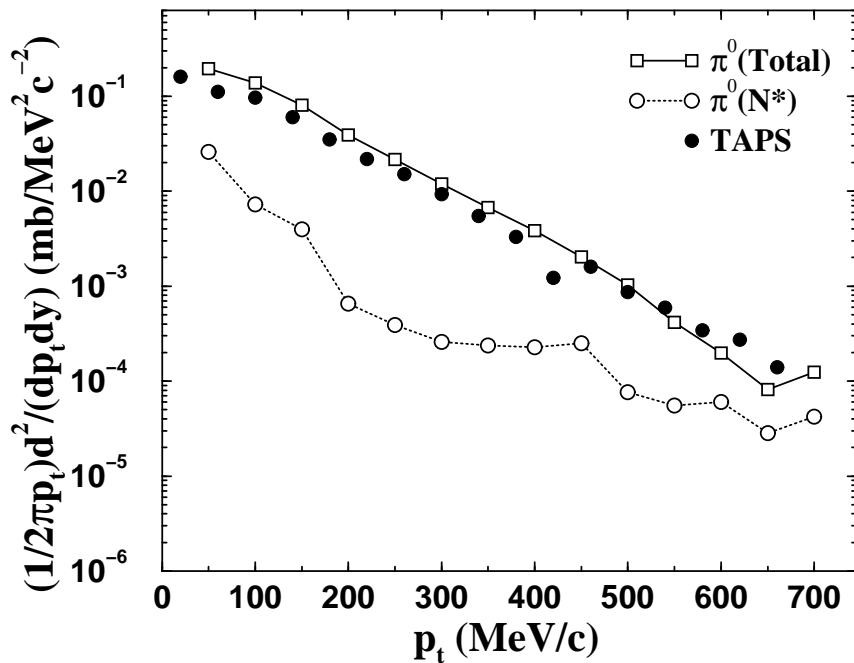


Fig. 7. Neutral pion p_t spectrum calculated with a Skyrme force (SMD) at midrapidity for a Au on Au reaction at 1 GeV/A under *minimum bias* condition is compared with the corresponding π^0 spectrum of pions originating from the decay of N^* -resonances. For comparison, TAPS data given in Ref. [11] is also shown. Due to a recent experimental analysis the data are renormalized by factor 0.6.

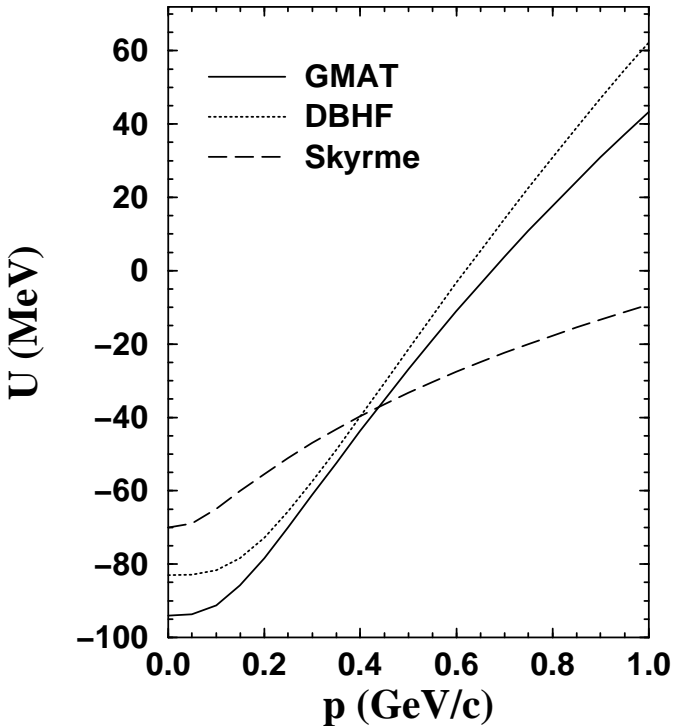


Fig. 8. The momentum dependence of nuclear single particle potential derived from the Brueckner G-matrix (GMAT) using the realistic Reid soft-core NN interaction is compared to the Skyrme interaction (SMD) at a density $\rho = \rho_o$. For comparison, also the potential obtained in Ref. [21] using the relativistic Dirac-Brueckner approach (DBHF) is shown.

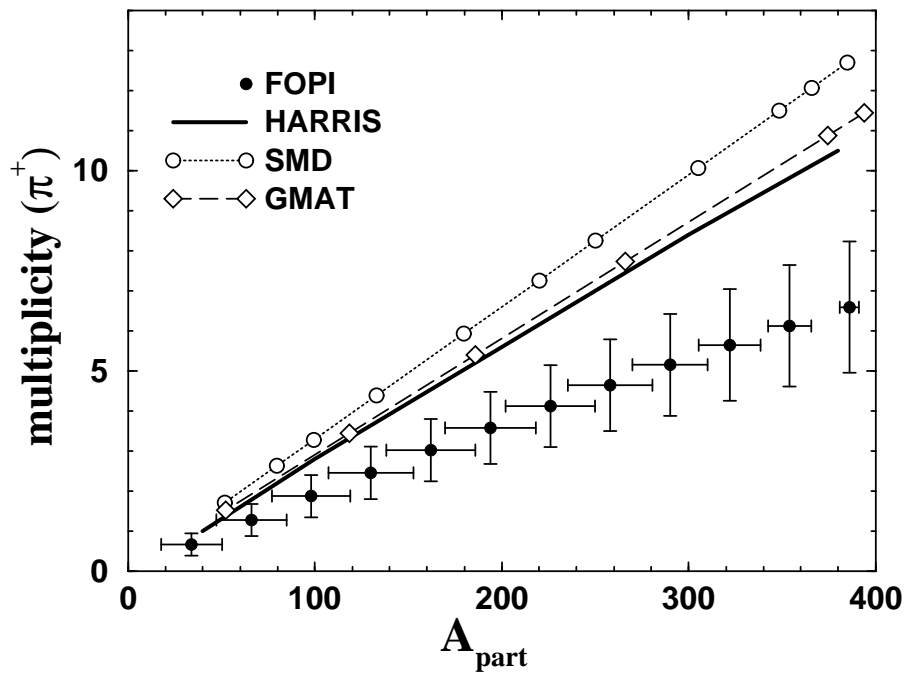


Fig. 9. The participant number dependence of π^+ multiplicity as obtained from the Brueckner G-matrix (GMAT) and a Skyrme force (SMD) are compared with the FOPI data [7]. In addition the experimentally derived Harris systematics [45] is shown.

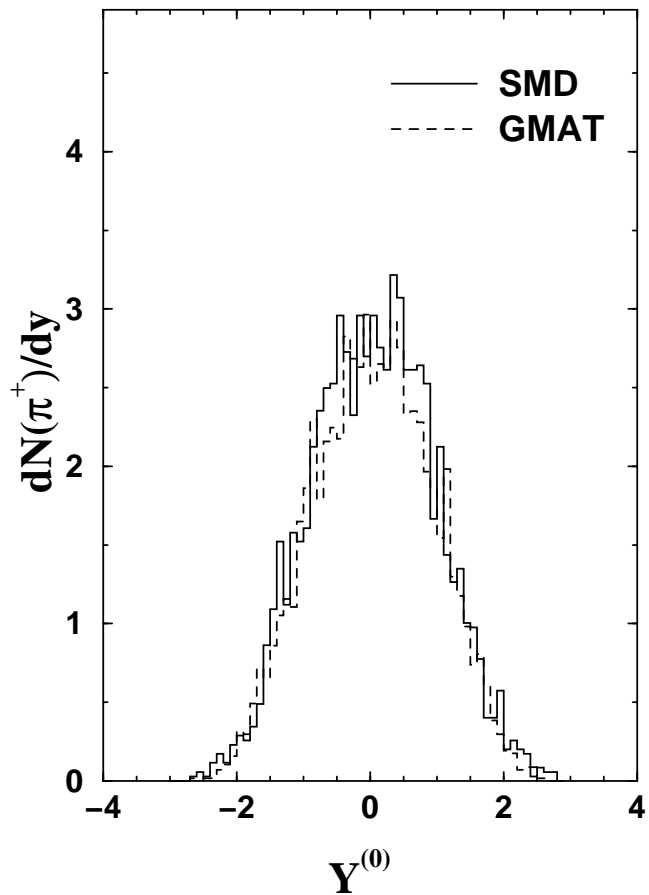


Fig. 10. The rapidity distributions of π^+ as obtained from the Brueckner G-matrix (GMAT) and a Skyrme force (SMD) is shown for transverse momenta $p_t > 0.1 \text{ GeV}/c$. The scaled c.m. rapidity $Y^{(0)} = Y/Y_{\text{proj}}$ is used.

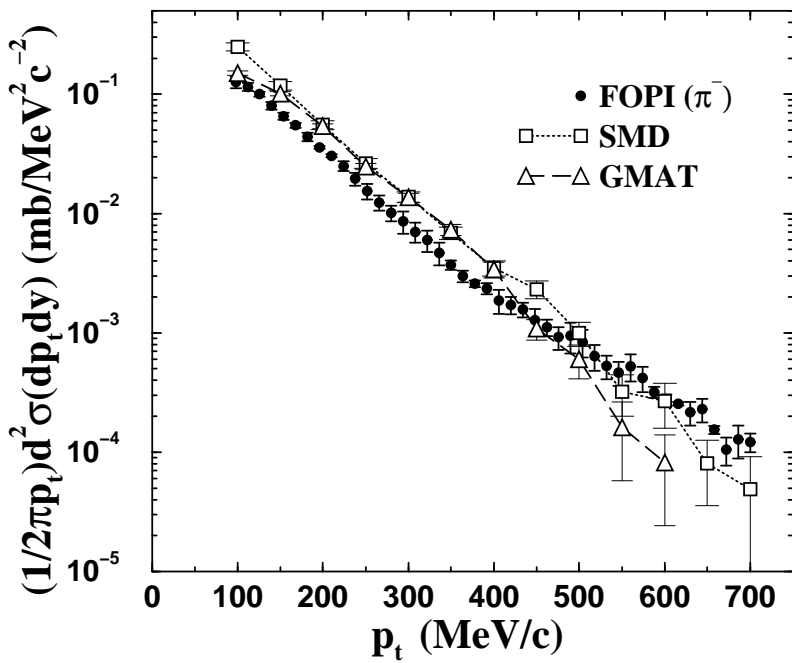


Fig. 11. The π^- p_t spectrum obtained at midrapidity in a Au on Au reaction at 1 GeV/A under *minimum bias* condition is compared to the FOPI data of Ref. [7].

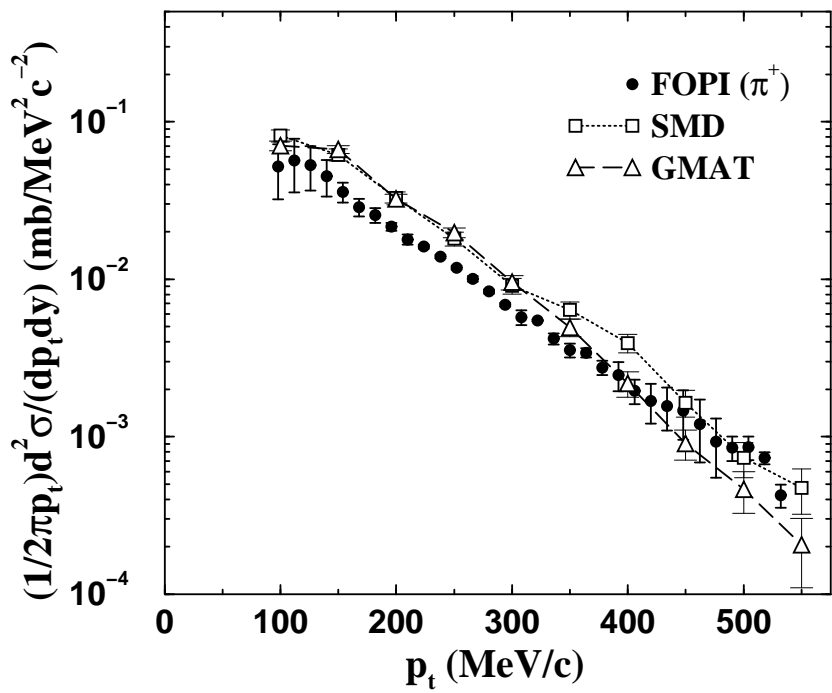


Fig. 12. Same as Fig. 11, but for π^+ .

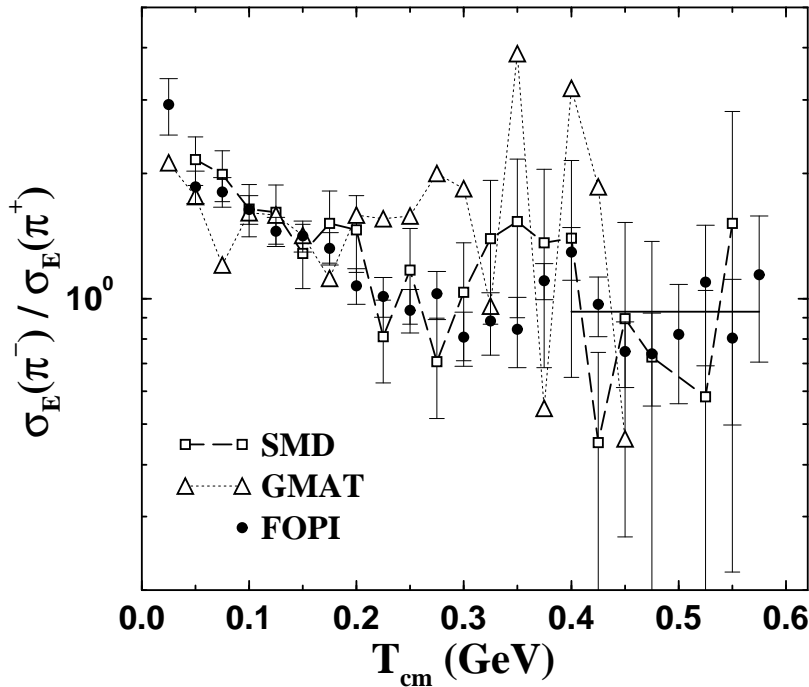


Fig. 13. The $\sigma_E(\pi^-)/\sigma_E(\pi^+)$ ratio calculated for the same reaction as in Fig.11. at midrapidity under *minimum bias* condition is shown as a function of the center-of-mass kinetic energy $T_{c.m.}$. The corresponding cross sections $\sigma_E = d^2\sigma/(pEdEd\Omega)$ are obtained with an angular cut $85^\circ < \Theta_{c.m.} < 135^\circ$. The data points are taken from the FOPI collaboration [7]. The horizontal solid line indicates that the observed π^-/π^+ ratio reaches a constant value of about 0.93 as pion energy increases.